Efficient self-consistent pseudopotential calculation of nanostructured devices

Francesco Chirico, Aldo Di Carlo, and Paolo Lugli
INFM–Dipartimento di Ingegneria Elettronica, Università di Roma ''Tor Vergata,'' 00133 Roma, Italy
(Received 10 July 2000; published 21 June 2001)

We have developed a full-band pseudopotential-based approach to describe semiconductor nanostructures. The method relies on the bulk Bloch functions expansion of the system wave function that guarantees an efficient integration of the full-band approach in self-consistent schemes where Schrödinger and Poisson equations are solved iteratively. In order to gain efficiency of the method a suitable separation between structure-dependent and material-dependent contributions to the system Hamiltonian is presented. Results are shown for typical nanostructures.

DOI: 10.1103/PhysRevB.64.045314 PACS number(s): 73.21.−b, 85.35.Be

I. INTRODUCTION

Nanostructures based on semiconductor heterojunctions are nowadays commonly used in electronic and optoelectronic devices. For instance, long-wavelength lasers for telecommunications may have active regions formed by a sequence of quantum wells obtained from the heterojunction of two or more semiconductors.[1] On the other hand, physical phenomena related to semiconductor nanostructures such as the confinement of electron in zero, one, and two dimensions are of great interest and have contributed to define new concepts in condensed matter physics.[2] A proper theoretical description of semiconductor nanostructures is thus of crucial importance since it allows us both to investigate fundamental physics and to optimize nanostructure-based devices.

Traditionally, nanostructures are studied via $\mathbf{k}\cdot\mathbf{p}$ approaches in the context of the envelope function approximation (EFA).[3] In this case, only the envelope of nanostructure wave function is described, regardless of atomic details. Despite the numerous assumptions involved,[4] envelope function approaches have obtained great success, mainly due to a fair compromise between the simplicity of the method and reliability of the results.

Modern applications, however, push nanostructures to dimensions and geometries where EFA may not be as accurate as one would need. This is for example the case of quantum dots,[5] strained δ layer,[6] or nanometer-scale silicon metal-oxide semiconductor field-effect transistors (MOSFET's).[7] In the latter case, oxide dimension, channel thickness, and channel length are such that the application of EFA is highly questionable.[8] On the other hand, however, as soon as the envelope function concept has to be substituted, for instance, by *ab initio* approaches, the complexity of the problem becomes rapidly intractable.

Ideally, one should try to combine a complete quantum-mechanical description based on a full-band approach, avoiding at the same time the computationally prohibitive load of the *ab initio* methods and the inherent physical limitations of the EFA. Moreover, charge rearrangement induced by the presence of externally applied or internally induced fields should be considered for a realistic description of the nanostructure. This is particularly true, for example, in nitride-based nanostructures whose properties strongly depend on the interplay between the internal fields induced by spontaneous and piezoelectric polarizations and the charge screening.[9]

Many different approaches have been developed to describe nanostructures beyond the $\mathbf{k}\cdot\mathbf{p}$ EFA. Localized basis approaches such as the tight-binding (TB) approach have been extensively used to predict optical and electronic properties of nanostructures.[10–18] In describing nanostructures, usually the empirical version of the TB is considered.[19,20] In this context, a parametrization of the hopping and on-site matrix elements is needed. Being a full-band approach, the TB approach overcomes the envelope function approximations and allows us to define atomic details, the realistic band structure in the whole Brillouin zone,[21] strain, and charge self-consistency.[22] Moreover, the computational cost of empirical TB approaches is close to that of $\mathbf{k}\cdot\mathbf{p}$ EFA approaches. The drawback of the empirical TB approach is the large number of parameters needed to accurately reproduce realistic band dispersions. These parameters need to be determined by a proper fitting of the bulk band structure obtained with other (more first-principle) methods. Moreover, transferability of these parameters should be required for a physical modeling of the TB Hamiltonian.

The empirical pseudopotential method (EPM) represents a higher level of sophistication. Few parameters are needed to define the pseudopotential, thus reducing the limitations of the TB approaches. However, the large number of plane waves needed to accurately describe the system even for the bulk case does not guarantee that such an approach can be easily extended to nanostructures where dimensions of hundreds of Å are typical.

The purpose of this article is to present a method that maintains both the degree of physical insight of full-band approaches and the speed of effective-mass models. We use, in fact, a physical starting point to describe the nanostructure, namely, the Bloch functions of the materials forming the nanostructure. These Bloch functions will be described in terms of local empirical pseudopotentials. We will show that a proper separation between material- and structure-dependent terms will lead to an efficient self-consistent solution of the Schrödinger and Poisson equations.

The use of the bulk Bloch function to describe nanostructures (as, in general, all the low-symmetry systems) is as old as the concept of envelope function approximation. Starting from the work of Kohn[23] for the description of impurity

states in semiconductors in terms of a bulk Bloch functions expansion [BBFE or linear combination of bulk bands (LCBB)], Altarelli developed the envelope function approach for semiconductor heterojunctions.[24,25] However, only at the end of the 1980s, did Burt[4] point out the full power of the BBFE, which allows one to correctly describe any effect contained in the pseudopotential description of the system.[26] Application of the bulk Bloch function expansion has been considered in the work on inversion layers in Si MOS by Fischetti and Laux.[8] Starting from the description in terms of empirical pseudopotentials of the inversion channel and applying the BBFE, they obtained, under certain approximations, a full-band solution of the problem. This approach without any approximation was later applied by Wang and co-workers[27] to the problem of Γ-X mixing in low-dimensional nanostructures containing as much as 10^6 atoms. The applicability of the method even in for the *ab initio* description of the problem has been addressed by Froyen.[28]

Our work differs from previous studies in the following points: (i) we will use the usual concept of the empirical pseudopotential where only few Fourier transform components of the pseudopotential are needed, avoiding any fitting procedure (Refs. 27 and 29), (ii) a Hamiltonian matrix element separation between material-dependent and structure-dependent terms will be developed, (iii) we will address the problem of the representation of an external potential and how to effectively couple the full-band approach to the Poisson equation, (iv) we will show that the problem of considering several materials can be solved via a generalized Schrödiner equation without requiring orthogonalization of the basis by-hand. The use of a nonorthogonalized basis is not strictly required (Refs. 27 and 29) but can be useful to establish fast convergence criteria.

II. THEORY

The one-electron Hamiltonian for a generic nanostructure in the presence of an external potential $V(\mathbf{r})$, is given by

$$\mathcal{H}=-\frac{\hbar^2}{2m}\nabla^2+\sum_{\sigma}\sum_{\alpha}W_{\alpha}^{\sigma}(\mathbf{r})V_{\alpha}^{\sigma}(\mathbf{r}-\mathbf{d}_{\alpha})+V(\mathbf{r})$$
$$=\mathcal{H}_1+\mathcal{H}_2+\mathcal{H}_3, \tag{1}$$

where σ is the material index, α is the atomic base index, $\mathbf{d}_{\alpha}$ is the offset of αth atom in the unit cell, $\mathbf{R}$ is the Bravais vector, and $V_{\alpha}^{\sigma}(\mathbf{r})$ is the (periodic) local atomic pseudopotential in real space related to the αth atom of the σ material. We are assuming that all materials constituting the structure have the same Bravais lattice although the approach can be generalized to strained materials.[29,28]

The weighting function $W_{\alpha}^{\sigma}(\mathbf{r})=W_{\alpha}^{\sigma}(\mathbf{R})$, where $\mathbf{r}=\mathbf{R}+\mathbf{r}_0$ with $\mathbf{r}_0$ inside the unit cell, contains the information about the composition of the system and is defined as

$$W_{\alpha}^{\sigma}(\mathbf{R})=\begin{cases}1 & \text{if the atom located at } \mathbf{R}+\mathbf{d}_{\alpha}\\ & \text{belongs to the } \sigma \text{ material}\\ 0 & \text{otherwise}\end{cases}$$

The three terms of the Hamiltonian in Eq. (1) represent, respectively, the kinetic term ($\mathcal{H}_1$), the crystal term ($\mathcal{H}_2$), and the external potential term ($\mathcal{H}_3$).

We expand the system wave function $\psi(\mathbf{r})$ over a linear combination of the bulk Bloch wave functions $\phi_{n\mathbf{k}}^{\sigma}(\mathbf{r})$ of all the materials forming the nanostructure

$$\psi(\mathbf{r})=\frac{1}{\sqrt{N}}\sum_{n\mathbf{k}\sigma}C_{n\mathbf{k}}^{\sigma}\phi_{n\mathbf{k}}^{\sigma}(\mathbf{r}), \tag{2}$$

where N is the number of unit cells in the large supercell that contains our nanostructure, n the band index, and $\mathbf{k}$ the wave vector. In a plane wave expansion, the bulk Bloch wave functions are written as

$$\phi_{n\mathbf{k}}^{\sigma}(\mathbf{r})=\langle\mathbf{r}|n\mathbf{k}\sigma\rangle=\frac{1}{\sqrt{\Omega_0}}\sum_{\mathbf{G}}B_{n\mathbf{k}}^{\sigma}(\mathbf{G})e^{i(\mathbf{G}+\mathbf{k})\cdot\mathbf{r}}, \tag{3}$$

with $\mathbf{G}$ the reciprocal lattice vector and Ω_0 the volume of the unit cell.

By using Eqs. (2) and (3) and assuming a proper representation of the external potential (see the Appendix), the Schrödinger equation for the nanostructure can be written as a generalized eigenvalue problem:[28]

$$\sum_{n\mathbf{k}\sigma}\mathcal{H}_{n'\mathbf{k}'\sigma',n\mathbf{k}\sigma}C_{n\mathbf{k}}^{\sigma}=E\sum_{n\mathbf{k}\sigma}\mathcal{S}_{n'\mathbf{k}'\sigma',n\mathbf{k}\sigma}C_{n\mathbf{k}}^{\sigma}, \tag{4}$$

where

$$\mathcal{H}_{n'\mathbf{k}'\sigma',n\mathbf{k}\sigma}=\langle n'\mathbf{k}'\sigma'|\mathcal{H}_1|n\mathbf{k}\sigma\rangle+\langle n'\mathbf{k}'\sigma'|\mathcal{H}_2|n\mathbf{k}\sigma\rangle$$
$$+\langle n'\mathbf{k}'\sigma'|\mathcal{H}_3|n\mathbf{k}\sigma\rangle \tag{5}$$

and

$$\mathcal{S}_{n'\mathbf{k}'\sigma',n\mathbf{k}\sigma}=\langle n'\mathbf{k}'\sigma'|n\mathbf{k}\sigma\rangle$$
$$=\delta_{\mathbf{k}\mathbf{k}'}\sum_{\mathbf{G}}B_{n'\mathbf{k}}^{\sigma'}(\mathbf{G})^*B_{n\mathbf{k}}^{\sigma}(\mathbf{G}) \tag{6}$$

represents the bulk wave-function overlap (equal to $\delta_{n'\mathbf{k}',n\mathbf{k}}$ only if $\sigma'=\sigma$).

The matrix element of each Hamiltonian term is given by

$$\langle n'\mathbf{k}'\sigma'|\mathcal{H}_1|n\mathbf{k}\sigma\rangle=\mathcal{A}_{n'\mathbf{k}'\sigma',n\mathbf{k}\sigma}$$
$$=\delta_{\mathbf{k}\mathbf{k}'}\sum_{\mathbf{G}}\frac{\hbar^2}{2m}|\mathbf{G}+\mathbf{k}|^2B_{n'\mathbf{k}}^{\sigma'}(\mathbf{G})^*B_{n\mathbf{k}}^{\sigma}(\mathbf{G}), \tag{7}$$

$$\langle n'\mathbf{k}'\sigma'|\mathcal{H}_2|n\mathbf{k}\sigma\rangle=\sum_{\alpha}\sum_{\sigma''}W_{\alpha}^{\sigma''}(\mathbf{k}-\mathbf{k}')\mathcal{B}_{n'\mathbf{k}'\sigma',n\mathbf{k}\sigma}^{\alpha\sigma''}, \tag{8}$$

$$\langle n'\mathbf{k}'\sigma'|\mathcal{H}_3|n\mathbf{k}\sigma\rangle=V(\mathbf{k}-\mathbf{k}')\mathcal{C}_{n'\mathbf{k}'\sigma',n\mathbf{k}\sigma}, \tag{9}$$

where $W_{\alpha}^{\sigma''}(\mathbf{k})$ and $V(\mathbf{k})$ are the discrete Fourier transform (DFT) of the W and V terms:

$$W_\alpha^{\sigma''}(\mathbf{k}) = \frac{1}{N} \sum_{\mathbf{R}} W_\alpha^{\sigma''}(\mathbf{R}) e^{i\mathbf{k}\cdot\mathbf{R}}, \tag{10}$$

$$V(\mathbf{k}) = \frac{1}{N} \sum_{\mathbf{R}} V(\mathbf{R}) e^{i\mathbf{k}\cdot\mathbf{R}}. \tag{11}$$

The $\mathcal{A}$, $\mathcal{B}$, $\mathcal{C}$, and $\mathcal{S}$ matrices (see the Appendix) depend on the material composition of the nanostructure and *do not depend on the particular geometry, sequence of layers, and potential profile of the nanostructure itself*. Thus, given a material set, $\mathcal{A}$, $\mathcal{B}$, $\mathcal{C}$, and $\mathcal{S}$ matrices can be precalculated and all the variation in geometry and/or in the external potential (as in typical self-consistent cycle) will require only the DFT of W and V. This is an essential separation since the time spent to calculate $\mathcal{A}$, $\mathcal{B}$, $\mathcal{C}$, and $\mathcal{S}$ may be large while that to obtain $W_\alpha^{\sigma''}(\mathbf{k})$ and $V(\mathbf{k})$ is negligible.

III. SELF-CONSISTENCY

Space-charge effects due to the electronic free-charge rearrangement can be included at a Hartree level by solving Poisson equation,

$$\nabla[\varepsilon(\mathbf{r}) \cdot \nabla V(\mathbf{r})] = -\rho(\mathbf{r}), \tag{12}$$

where $\varepsilon(\mathbf{r})$ is the position-dependent dielectric constant.[22] Here we consider only the free-charge contribution to the Hartree potential, that is, electrons in the conduction band and/or holes in the valence band, and we neglect the valence electrons that are accounted for (non-self-consistently) in the dielectric constant.

By using Eqs. (2) and (3), we obtain the real-space representation of $|\psi(\mathbf{r})|^2$:

$$|\psi(\mathbf{r})|^2 = \frac{1}{N\Omega_0} \sum_{\sigma' n' \mathbf{k}'} \sum_{\sigma n \mathbf{k}} C_{n'\mathbf{k}'}^{\sigma'} {}^* C_{n\mathbf{k}}^{\sigma} \times \left[\sum_{\mathbf{G}} \sum_{\mathbf{G}'} B_{n'\mathbf{k}'}^{\sigma'}(\mathbf{G}') {}^* B_{n\mathbf{k}}^{\sigma}(\mathbf{G}) e^{i(\mathbf{G}-\mathbf{G}'+\mathbf{k}-\mathbf{k}')\cdot\mathbf{r}} \right]. \tag{13}$$

The term in square bracket is independent of structure and, for a particular choice of the materials forming the nanostructure, can be calculated, stored, and than used for other geometries as long as the materials are the same.

From the expression of the squared wave function one can obtain the charge density at each position. It is, however, necessary to consider explicitely the symmetry of the system. It is always possible to define a unit cell of the (bulk) materials forming the nanostructure in such a way that some basis vectors belong to the ''perpendicular'' space, where the translational symmetry of the system is broken and the rest of the basis vectors belong to the ''parallel'' space, where the full periodicity of the crystal is preserved. A given Bravais vector can thus be decomposed into perpendicular and parallel components: $\mathbf{R} = \mathbf{R}_\perp + \mathbf{R}_{||}$. For $\mathbf{R}_{||}$, a reciprocal parallel space can be defined and consequently the Brillouin zone $\mathrm{BZ}_{||}$ for the $\mathbf{k}_{||}$ vectors (with $\mathbf{k} = \mathbf{k}_\perp + \mathbf{k}_{||}$). In the case of a dot, where the translational symmetry is lost in all three dimensions, the parallel space will be empty and the perpendicular space will coincide with the Bravais lattice ($\mathbf{R} = \mathbf{R}_\perp$).

In order to reduce the microscopic oscillation between atomic planes a macroscopic average similar to that used in band-offset calculations[30] is considered. By writing $\mathbf{r} = \mathbf{r}_0 + \mathbf{R}_\perp$ in Eq. (13), with $\mathbf{r}_0$ inside the unit cell, we can integrate over the unit cell volume obtaining

$$|\psi(\mathbf{R}_\perp, \mathbf{k}_{||})|^2 = \frac{1}{N} \sum_{\sigma' n' \mathbf{k}'} \sum_{\sigma n \mathbf{k}} C_{n'\mathbf{k}'}^{\sigma'} {}^* C_{n\mathbf{k}}^{\sigma} e^{i(\mathbf{k}-\mathbf{k}')_\perp \cdot \mathbf{R}_\perp} \times \left[\sum_{\mathbf{G}} \sum_{\mathbf{G}'} B_{n'\mathbf{k}'}^{\sigma'}(\mathbf{G}') {}^* B_{n\mathbf{k}}^{\sigma}(\mathbf{G}) \delta_{\mathbf{G}_{||}, \mathbf{G}'_{||}} \times \mathrm{sinc}(\mathbf{G}_\perp + \mathbf{k}_\perp - \mathbf{G}'_\perp - \mathbf{k}'_\perp) \right]. \tag{14}$$

The above expression is general and can be used regardless of the degree of quantization in the system, provided that the proper definition of perpendicular and parallel space is given. In the above expression, we have averaged in the whole unit cell; however, a smaller portion of the unit cell may be considered without introducing microscopic oscillations of the charge density. For a [001] grown zinc-blende structure one can average the two adjacent anion-cation planes in the $\mathbf{R}_\perp$ direction and eliminate the microscopic oscillations.[13]

The charge density $\rho(\mathbf{R}_\perp)$ is defined as

$$\rho(\mathbf{R}_\perp) = -\frac{e}{(2\pi)^D} \int_{\mathrm{BZ}_{||}} d\mathbf{k}_{||} \sum_{\nu} |\psi(\mathbf{R}_\perp, \mathbf{k}_{||}, E_\nu)|^2 \tilde{f}(E_\nu), \tag{15}$$

where e is the electron charge, ν labels the energy levels (E_ν) for a given $\mathbf{k}_{||}$, and D is the dimensionality of the parallel space. The function $\tilde{f}(E_n, E_F)$ is defined as follows:

$$\tilde{f}(E_\nu) = \begin{cases} f(E_\nu, E_F^c) & \text{for the conduction states} \\ 1 - f(E_\nu, E_F^v) & \text{for the valence states,} \end{cases} \tag{16}$$

where $f(E_\nu, E_F)$ is the Fermi distribution function for a given quasi-Fermi-level E_F. Electron and hole quasi-Fermi-levels, E_F^c and E_F^v, respectively, are different if the system is out of equilibrium as in the case optical of electrical injection. At finite temperatures, $\tilde{f}(E_\nu, E_F)$ is in any case a well-behaved function that is different from zero only in the proximity of the valence and conduction band edges.

The Poisson and Schrödinger equations [Eqs. (12) and (4), respectively] are iteratively solved until convergence is reached. To speed up the convergence we use a first-order expansion of the method presented in Ref. 31.

As already pointed out in the previous section, the efficiency of the self-consistent procedure is based on the separability between the contributions to the Hamiltonian coming from external potential and the material. Indeed, the Fourier transform of the external potential is the only quantity that needs to be calculated in each self-consistent cycle.

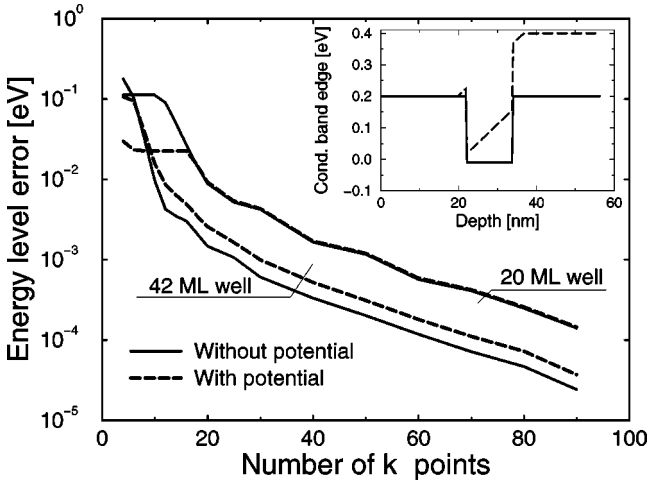

FIG. 1. Calculated error for the first quantized energy level in the AlAs/GaAs quantum well as a function of the number of *k* points (i.e., number of bulk Bloch wave functions for each material and each band) considered in the calculation. Results are shown for a well width of 42 and 20 ML with and without the application of an external potential. Here $\mathbf{k}_{\|}=\mathbf{0}$. Inset: The conduction band profile of the nanostructure around the quantum well when the external potential is applied.

IV. APPLICATION OF THE FULL-BAND PROCEDURE TO ONE-DIMENSIONAL NANOSTRUCTURES

As a matter of example, we restrict ourselves to a situation where the symmetry is broken in one direction, which is typical for many nanostructures such as superlattices, quantum wells, or channels in high-electron-mobility transistors (HEMT's). In the following calculation we use empirical local pseudopotential taken from Ref. 32.

A. GaAs quantum well and convergence of the method

In order to test the method and to define convergence criteria we have applied the full-band approach to a AlGa/GaAs quantum well with several well widths. We consider the AlAs/GaAs system grown in the [001] direction and we choose for the unit cell of the semiconductors forming the heterojunction the following basis:

$$\mathbf{R}_1=a(0.5,0.5,0),$$

$$\mathbf{R}_2=a(-0.5,0.5,0),$$

$$\mathbf{R}_3=a(0,0,1). \tag{17}$$

The translational symmetry is broken only in the $\mathbf{R}_3$ direction, allowing an easy separation between the perpendicular ($\mathbf{R}_{\perp}=n\mathbf{R}_3$) and parallel ($\mathbf{R}_{||}=m\mathbf{R}_1+l\mathbf{R}_2$) spaces. The energy offset between Γ_{GaAs} and X_{AlAs} has been set to 204 meV. The system has a total width of 56.5 nm. We consider two cases with and without the application of an external potential. The external potential consists of a linear potential drop of 0.2 V in the well region (resulting in a electric field of 120 kV/cm), as shown in the inset of Fig. 1.

Figure 1 shows the calculated absolute error of the first quantized energy level of the conduction band as a function of number of $\mathbf{k}_{\perp}$ points (*k* points) included in the expansion, Eq. (2) (here $\mathbf{k}_{\|}=\mathbf{0}$) for a well width of 42 and 20 monolayers (1 ML=2.83 Å), respectively. In the [001] direction, the Brillouin zone of the bulk materials has been divided in 100 *k* points, the total width of the system being $100R_3$. Thus, the number of *k* points refers to the *k* points *around* Γ included in the calculation. The *k* point expansion is thus centered around Γ, which is the minimum conduction band (we recall the fact that, according to the choice of the unit cell, we are working with folded bands). A better choice of *k* points can, however, be obtained by picking up only those points that do really contribute to the expansion. The error has been calculated by comparing the result with that obtained with four bands and 100 *k* points. The results shown have been obtained considering two conduction bands for each material in the bulk-band expansion. We do not find significant differences in the results including a larger number of bands as long as the number of *k* points included is large enough (>10).

A close inspection of Fig. 1 reveals that the number of *k* points needed to achieve results within 1 meV of error is structure dependent.[27] For the larger quantum well we need around 30 *k* points while we need 50 *k* points for the smaller one. Moreover, the presence of an external potential defines a minimum requirement of *k* points for the Fourier representation of the potential itself. In fact, we notice from Fig. 1 that, for the larger well, the presence of the external potential implies the use of a larger number of *k* points in order to achieve the same convergence level with respect to the case without an external potential. For the smaller well, the number of *k* points needed to achieve convergence in the absence of an external potential suffices for the representation of the external potential when applied.

B. Confining potentials and one material approximation

In many situations it may be a good approximation to represent a heterojunction by using a single material and applying a confining potential to mimic the presence of the band discontinuity. This could be the case of $\mathrm{GaAs/Al}_x\mathrm{Ga}_{1-x}\mathrm{As}$ structures with low Al concentrations where the difference between the electron masses of the two materials at the Γ point of the conduction band may be neglected. A similar situation occurs in all the cases where the presence of the heterojunction can be represented by proper boundary conditions. As a matter of example, in silicon MOS structures the $\mathrm{SiO_2/Si}$ band discontinuity is very large and we can reasonably assume that the wave function of the electron vanishes at the interface between silicon and oxide (infinite barrier approximation).[8,33] In all these situations Eqs. (6)–(8) can be greatly simplified in the following way,

$$\mathcal{S}_{n'\mathbf{k}'\sigma',n\mathbf{k}\sigma}=\delta_{\mathbf{k}\mathbf{k}'}\delta_{nn'} \tag{18}$$

and

$$\langle n'\mathbf{k}'|\mathcal{H}_1+\mathcal{H}_2|n\mathbf{k}\rangle=E_{n\mathbf{k}}\delta_{\mathbf{k}\mathbf{k}'}\delta_{nn'}, \tag{19}$$

where $E_{n\mathbf{k}}$ is the bulk energy dispersion of the material. By using this simplified expression we can write the full-band Schrödinger equation as

$$\sum_{n'\mathbf{k}'} [E_{n\mathbf{k}}\delta_{\mathbf{k}\mathbf{k}'}\delta_{nn'} + V(\mathbf{k}-\mathbf{k}')\mathcal{C}_{n'\mathbf{k}',n\mathbf{k}}]C_{n'\mathbf{k}'} = EC_{n\mathbf{k}}. \tag{20}$$

Thus, the full-band results can be obtained from the knowledge of the band dispersion and the $\mathcal{C}$ coefficients.

It should be noticed that if in Eq. (20) we approximate $\mathcal{C}_{n'\mathbf{k}',n\mathbf{k}} = \delta_{\mathbf{k}\mathbf{k}'}\delta_{nn'}$ we obtain the equation reported by Fischetti and Laux.[8] In order to justify this approximation we have calculated the $\mathcal{C}$ terms for the case of silicon. We found that $\mathcal{C}_{n'\mathbf{k}',n\mathbf{k}} \simeq \mathcal{C}_{n\mathbf{k}',n\mathbf{k}}\delta_{nn'}$ (with an off-diagonal component several order of magnitude lower than the diagonal one). The value of $\mathcal{C}_{n\mathbf{k}',n\mathbf{k}}$ for the first conduction band range between 0.9 and 1.0. Thus we can conclude that the approximation of Ref. 8 is well justified within 10% of error.

C. Self-consistent results for a AlAs/GaAs HEMT

In this last section, we consider the self-consistent full-band result for a AlAs/GaAs HEMT-like structures. Let us consider the unit cell defined in Sec. IV A. The two-dimensional Brillouin zone has an irreducible wedge (IW) defined by

$$0 \leqslant k_x < \frac{2\pi}{a}, \quad 0 \leqslant k_y < \min\left(k_x, \frac{2\pi}{a} - k_x\right). \tag{21}$$

The $\mathbf{k}_\parallel$ integration needed to calculate the charge density Eq. (15), is obtained by using a special k point sampling[34] of the irreducible wedge. However, only a small portion of the irreducible wedge will contribute to the density, formed by the conduction band states (or valence band states when considered) close to Fermi level. Thus, in order to reduce the computation effort, we select only those points of the IW belonging to these most significative regions. We have found that convergent results can be obtained with a small number of special k points in these regions. For instance, in the AlAs/GaAs case, we obtain convergence for by using three $\mathbf{k}_\parallel$ points with $|\mathbf{k}_\parallel| < 0.06$ and 18 $\mathbf{k}_\parallel$ points with $|\mathbf{k}_\parallel - (0,0.85)| < 0.2$ (here we use $2\pi/a$ units).

The self-consistent procedure has not been applied directly to the AlAs/GaAs quantum well. In fact the dimension of a typical HEMT will be of the order of several microns and the potential will vary over this scale. Boundary conditions should be imposed at the real edges of the devices. However, electrons will accumulate mainly in the quantized channel. In order to be able to handle the problem, we have use an embedded calculation: the whole structure is divided into a quantum region where the full-band approach is considered and in a semiclassical region where quantization effects are not present. In the latter region a classical three-dimensional Thomas-Fermi description is used to calculate the electron density (if present) and ionized doping density.

The structure we have considered consists of an AlAs buffer, 42 ML of GaAs forming the quantum well, and 131 ML of AlAs ending with a metal to form the Schottky contact (with a barrier high of $\phi_B = 0.8$eV). We choose a quantum region of 200 ML (56.5 nm) centered around the quantized channel (GaAs) while the total width of the device is 3 μm. The top 35 nm layer of AlAs close to the Schottky contact is n-doped with $N_D = 2\times10^{18}$ cm^{-3}. The one-dimensional Poisson equation, Eq. (12), is solved using a fixed potential at the metal-AlAs contact equal to the ϕ_B plus the gate bias (if applied) while the zero-field condition is imposed at the opposite end of the structure. According to the discussion of Sec. IV A we choose 61 k points and two conduction bands in the bulk band expansion for each semiconductor.

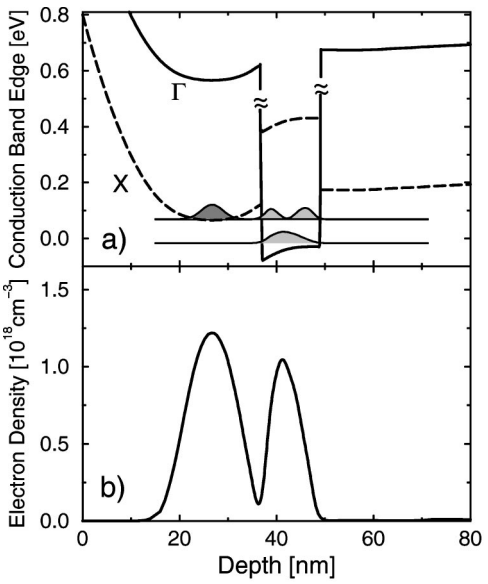

FIG. 2. (a) Self-consistent conduction band edge profile of the AlAs/GaAs HEMT-like structure for the Γ and X valley. The first three squared envelope wave functions are also shown. The zero of the envelope corresponds to the energy of the quantized level. Here $E_F = 0$. (b) Electron charge density in the nanostructure.

Figure 2(a) shows the calculated conduction band envelope at Γ and X points. Also depicted are the first three envelope squared wave functions where the zero of each wave function has been set to the energy of the corresponding energy level. The total electron density is shown in Fig. 2(b). Electron confinement occurs both in the well and in the barrier. The former is related to the GaAs Γ conduction band minimum while the barrier states are those arising from the X states of the AlAs. The electron density is spread over the real GaAs channel and over the *parasitic* AlAs channel. The presence of the parasitic channel has negative influence in the HEMT performance and should be reduced as much as possible. Electron in the parasitic AlAs channel are also quantized. On the right end they are confined by the AlAs/GaAs barrier and on the left side by the potential profile. However, due both to the large effective masses of the AlAs conduction minima and to the extension of the confining region the energy quantization is quite small. We should point out that the integration in the 2D Brillouin zone in $\mathbf{k}_\parallel = (0,0)$ and $\mathbf{k}_\parallel = (0,0.85)2\pi/a$ represents the two situations

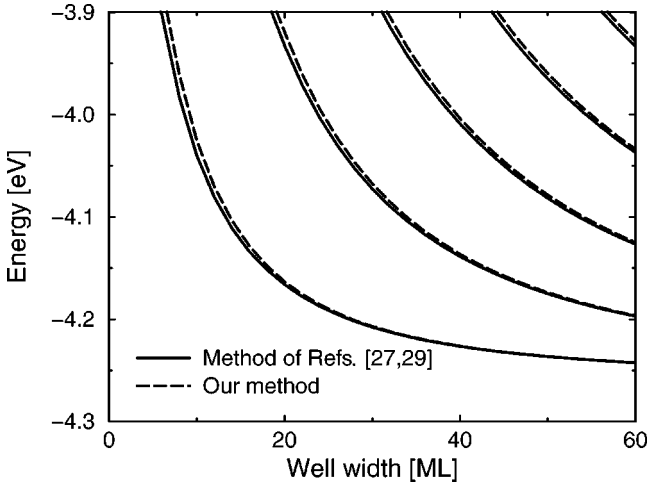

FIG. 3. Comparison between our method and the one of Refs. 27 and 29 for a AlAs/GaAs quantum well as a function of well width. An abrupt interface is considered.

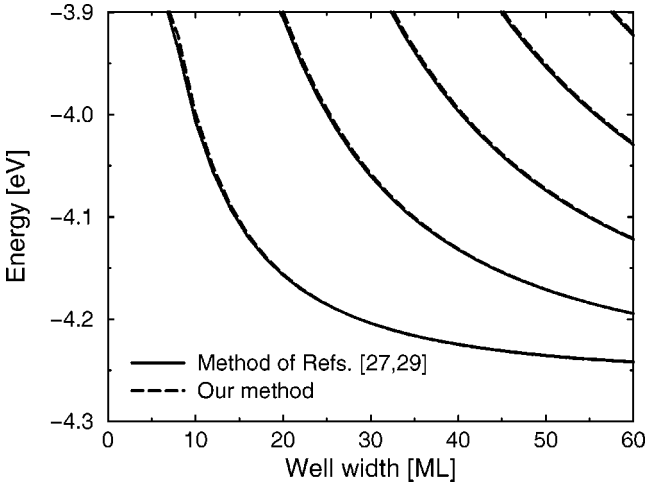

FIG. 4. Comparison between our method and the one of Refs. 27 and 29 for a AlAs/GaAs quantum well as a function of well width. An 2 ML smoothed interface is considered.

where quantization arises from electrons with longitudinal mass and from electrons with transversal mass in the X valleys, respectively.

Finally, we would like to address the question about the computational load of such calculations. Starting from a classical initial guess of the potential profile, the final result is obtained in circa 10 self-consistent cycles. The overall calculation is achieved in one hour on a typical single-processor workstation. The calculation of the $\mathcal{A}$, $\mathcal{B}$, $\mathcal{C}$, and $\mathcal{S}$ matrix elements is much more expansive and may require many hours of computation. However, as discussed in the previous sections, such matrix elements need to be calculated only once. Moreover, the structure of such matrix elements calls for a straightforward parallelization where each element of the matrix can be calculated on a different processor.

D. Comparison with other approaches

In the following we will briefly compare our approach with the one of Refs. 27 and 29 (hereafter called LCBB). In the LCBB method one needs to know the form of the pseudopotential in all of the reciprocal space up to certain cutoff. This can be obtained with fitting procedures (see, for example, Ref. 35). In contrast, our approach is based on the spirit of the usual empirical pseudopotential theory where only few Fourier transform components of the pseudopotential (for few G) are needed. This allows us to use all the empirical pseudopotential parameterizations developed so far. The drawback of our method concerns the treatment of the interface. At the interface we change abruptly the periodic pseudopotential. However, this error is negligible if we consider a smooth interface or a large nanostructure as we will show in the following.

We have calculated the electronic properties of a AlAs/GaAs quantum well with our approach and the LCBB method. We use the pseudopotential of Ref. 35. Figures 3 and 4 show the energy of the conduction band confined states in the well as a function of the well width. Figure 3 represents the results for an abrupt interfaces while Fig. 4 represents the results for a smooth interfaces with a 2 ML transition region between the two materials. In the transition region we use a linear interpolation of the two pseudopotentials.

For a narrow quantum well (10 ML) we obtain a maximum difference between our method and the LCBB method of about 15 meV for the abrupt interface case, which reduces to 5 meV in the smooth interface case. The discrepancy between the two methods reduces drastically ($\approx$1 meV) by increasing the size of the well, and it is of the order of 1 meV for the results of the previous sections. We should point out, as discussed in Refs. 27 and 29, that bulk-band expansion methods are suited for large nanostructure description while full diagonalization methods can be used for small nanostructures.

V. CONCLUSIONS

We have developed a full-band pseudopotential-based approach to describe semiconductor nanostructures. The method based on the Bloch band expansion of the system wave function allows us for an integration in a self-consistent scheme. To perform such integrations we have made a suitable separation between structure-dependent and material-dependent contributions to the system Hamiltonian. The efficency of the full-band self-consistent approach has been demonstrated for AlAs/GaAs high-electron-mobility transistor structures, showing how relaxation of any envelope function approximation can be achieved even at the self-consistent level without making the problem computationally intractable.

ACKNOWLEDGMENTS

We would like to thank Dr. F. Della Sala and Dr. M. Povolotskyi for stimulating discussion about bulk-band expansion methods. This work has been partially funded by MURST, CNR progetto 5% Microelettronica, and by the Office of Naval Research.

APPENDIX: MATRIX ELEMENTS

The coefficient for the crystal potential part of the Hamiltonian ($\mathcal{H}_2$) can be easily obtained by direct evaluation of the matrix element in Eq. (8):

$$\mathcal{B}^{\alpha\sigma''}_{n'\mathbf{k}'\sigma',n\mathbf{k}\sigma}=\left\{\sum_{\mathbf{G},\mathbf{G}',\mathbf{G}''} B^{\sigma'}_{n'\mathbf{k}'}(\mathbf{G}')^* B^{\sigma}_{n\mathbf{k}}(\mathbf{G}) V^{\sigma''}_{\alpha}(\mathbf{G}'') \times e^{-i\mathbf{G}''\cdot\mathbf{d}_\alpha}\,\mathrm{sinc}(\mathbf{G}+\mathbf{G}''-\mathbf{G}'+\mathbf{k}-\mathbf{k}')\right\}, \tag{A1}$$

where

$$\mathrm{sinc}(\mathbf{G}+\mathbf{G}''-\mathbf{G}'+\mathbf{k}-\mathbf{k}')=\mathrm{sinc}(\alpha_1)\mathrm{sinc}(\alpha_2)\mathrm{sinc}(\alpha_3), \tag{A2}$$

with $\mathrm{sinc}(\alpha_i)=\sin(\pi\alpha_i)/(\pi\alpha_i)$. The real coefficients $\alpha_i, i=1,\ldots,3$ are defined by

$$\mathbf{G}+\mathbf{G}''-\mathbf{G}'+\mathbf{k}-\mathbf{k}'=\alpha_1\mathbf{G}_1+\alpha_2\mathbf{G}_2+\alpha_3\mathbf{G}_3, \tag{A3}$$

where $\mathbf{G}_1,\mathbf{G}_2,\mathbf{G}_3$ are the reciprocal lattice basis.

For the external potential term ($\mathcal{H}_3$, we must define a reasonable approximation that makes the matrix element separable in two parts: one that is potential dependent but easy to calculate, and the second that is potential independent. In the following we discuss two complementary approximations.

The expression for the potential matrix element is

$$\langle n'\mathbf{k}'\sigma'|\mathcal{H}_3|n\mathbf{k}\sigma\rangle=\frac{1}{\Omega}\int_\Omega d\mathbf{r}\sum_{\mathbf{G}}\sum_{\mathbf{G}'} V(\mathbf{r})e^{i(\mathbf{G}+\mathbf{k}-\mathbf{G}'-\mathbf{k}')\cdot\mathbf{r}} \times B^{\sigma'}_{n'\mathbf{k}'}(\mathbf{G}')^* B^{\sigma}_{n\mathbf{k}}(\mathbf{G}). \tag{A4}$$

If we consider that the potential is constant inside the unit cell [i.e., $V(\mathbf{R}+\mathbf{r}_0)\equiv V(\mathbf{R})$ for $\mathbf{r}_0$ varying in the unit cell], we obtain

$$\langle n'\mathbf{k}'\sigma'|\mathcal{H}_3|n\mathbf{k}\sigma\rangle=V(\mathbf{k}-\mathbf{k}') \times\sum_{\mathbf{G}}\sum_{\mathbf{G}'} B^{\sigma'}_{n'\mathbf{k}'}(\mathbf{G}')^* B^{\sigma}_{n\mathbf{k}}(\mathbf{G})\frac{1}{\Omega_0} \times\int_{\Omega_0} e^{i(\mathbf{G}+\mathbf{k}-\mathbf{G}'-\mathbf{k}')\cdot\mathbf{r}_0}d\mathbf{r}_0 \tag{A5}$$

with

$$V(\mathbf{k})=\frac{1}{N}\sum_{\mathbf{R}} V(\mathbf{R})e^{i\mathbf{k}\cdot\mathbf{R}}. \tag{A6}$$

If we decompose $\mathbf{G}+\mathbf{k}-\mathbf{G}'-\mathbf{k}'=\alpha_1\mathbf{G}_1+\alpha_2\mathbf{G}_2+\alpha_3\mathbf{G}_3$ and $\mathbf{r}_0=\beta_1\mathbf{R}_1+\beta_2\mathbf{R}_2+\beta_3\mathbf{R}_3$ with α_i and β_i real numbers and $\mathbf{R}_i$ the Bravais lattice basis, we finally have the form of Eq. (9) with

$$\mathcal{C}_{n'\mathbf{k}'\sigma',n\mathbf{k}\sigma}=\sum_{\mathbf{G}}\sum_{\mathbf{G}'} B^{\sigma'}_{n'\mathbf{k}'}(\mathbf{G}')^* B^{\sigma}_{n\mathbf{k}}(\mathbf{G})e^{i\pi(\alpha_1+\alpha_2+\alpha_3)} \times\mathrm{sinc}(\alpha_1)\mathrm{sinc}(\alpha_2)\mathrm{sinc}(\alpha_3), \tag{A7}$$

in the direction G_i where the potential does not change, α_i is an integer number and $\mathrm{sinc}(\alpha_i)=\delta_{\alpha_i}$.

Another kind of separability can be obtained if the potential varies smoothly in the space. In this case we can consider that the Fourier transform of the potential is limited to the first Brillouin zone (BZ) related to the unit cell choose. So, if we assume that the following relation holds,

$$V(\mathbf{k})=\begin{cases} V(\mathbf{k}) & \text{for } \mathbf{k}\in\mathrm{BZ} \\ 0 & \text{otherwise}\end{cases} \tag{A8}$$

we can than use the sampling theorem to express $V(\mathbf{r})$ in a more convenient way:

$$V(\mathbf{r})=\sum_{\mathbf{R}} V(\mathbf{R})\mathrm{sinc}\left(\frac{\mathbf{G}_1}{2\pi}\cdot(\mathbf{r}-\mathbf{R})\right)\mathrm{sinc}\left(\frac{\mathbf{G}_2}{2\pi}\cdot(\mathbf{r}-\mathbf{R})\right) \times\mathrm{sinc}\left(\frac{\mathbf{G}_3}{2\pi}\cdot(\mathbf{r}-\mathbf{R})\right). \tag{A9}$$

By using this expression in Eq. (A4) we obtain the separability between the Fourier transform of the potential and the material depend part [Eq. (9)] with

$$\mathcal{C}_{n'\mathbf{k}'\sigma',n\mathbf{k}\sigma}=\left\{\sum_{\mathbf{G}}\sum_{\mathbf{G}'}\mathrm{Rect}_{\mathbf{G}_1,\mathbf{G}_2,\mathbf{G}_3}(\mathbf{G}+\mathbf{k}-\mathbf{G}'-\mathbf{k}') \times B^{\sigma'}_{n'\mathbf{k}'}(\mathbf{G}')^* B^{\sigma}_{n\mathbf{k}}(\mathbf{G})\right\}, \tag{A10}$$

where

$$\mathrm{Rect}_{\mathbf{G}_1,\mathbf{G}_2,\mathbf{G}_3}(\mathbf{G}+\mathbf{k}-\mathbf{G}'-\mathbf{k}') \times\begin{cases}1 & \text{for } (\mathbf{G}+\mathbf{k}-\mathbf{G}'-\mathbf{k}')\in\mathrm{BZ} \\ 0 & \text{otherwise.}\end{cases} \tag{A11}$$

Within this approximation we limit the potential in k space; however, the real-space shape will vary smoothly avoiding the step profile of the other case.

The use of the forms in Eq. (A7) or Eq. (A10) for the $\mathcal{C}$ coefficient will depend on the problems we have to solve. Typically in a self-consistent scheme the potential varies slowly and the form of Eq. (A10) is preferred. On the other hand, if the potential is used to mimic a band discontinuity, than the form in Eq. (A7) should be considered.

[1] A. Yariv, *Optical Electronics in Modern Communications* (Oxford University Press, New York, 1997).
[2] J.H. Davies, *The Physics of Low-Dimensional Semiconductors: An Introduction* (Cambridge University Press, UK, 1997).
[3] G. Bastard, *Wave Mechanics Applied to Semiconductor Heterostructures* (Les Edition de Physique, Les Ulis, 1988).
[4] M.G. Burt, J. Phys.: Condens. Matter **4**, 6651 (1992); **11**, R53 (1999).
[5] A. Mizel and M.L. Cohen, Phys. Rev. B **57**, 9515 (1998).
[6] F. Seiferth, F.G. Johnson, S.A. Merrit, S. Fox, R.D. Whaley, Y.J. Chen, M. Degenais, and D.R. Stone, IEEE Photonics Technol. Lett. **9**, 1340 (1997); A. Di Carlo, A. Reale, L. Tocca, and P. Lugli, IEEE J. Quantum Electron. **34**, 1730 (1998).
[7] Hon-Sum Philip Wong, D.J. Frank, P.M. Solomon, C.H.J. Wann, and J.J. Welser, Proc. IEEE **87**, 537 (1999).
[8] M.V. Fischetti and S.E. Laux, Phys. Rev. B **48**, 2244 (1993).
[9] F. Della Sala, A. Di Carlo, P. Lugli, F. Bernardini, V. Fiorentini, R. Scholz, and J.M. Jancu, Appl. Phys. Lett. **74**, 2002 (1999); A. Di Carlo, F. Della Sala, P. Lugli, V. Fiorentini, and F. Bernardini, *ibid.* **76**, 3950 (2000).
[10] T.B. Boykin, J.P.A. van der Wagt, and J.S. Harris, Phys. Rev. B **43**, 4777 (1991); T.B. Boykin Phys. Rev. B **51**, 4289 (1995).
[11] S.K. Kirby, D.Z.-Y. Ting, and T.C. McGill, Phys. Rev. B **48**, 15 237 (1993).
[12] M.S. Kiledjian, J.N. Schulman, K.L. Wang, and K.V. Rousseau, Phys. Rev. B **46**, 16 012 (1992).
[13] J.N. Schulman and Y.C. Chang, Phys. Rev. B **31**, 2056 (1985).
[14] G. Armelles and V.R. Velasco, Phys. Rev. B **54**, 16 428 (1996).
[15] I.A. Papadogonas, A.N. Andriotis, and E.N. Economou, Phys. Rev. B **55**, 10 760 (1997).
[16] M. Di Ventra and A. Baldereschi, Phys. Rev. B **57**, 3733 (1998).
[17] D. Porezag, Th. Frauenheim, Th. Köhler, G. Seifert, and R. Kaschner, Phys. Rev. B **51**, 12 947 (1995); M. Elstner, D. Porezag, G. Jungnickel, J. Elsner, M. Haugk, Th. Frauenheim, S. Suhai, and G. Seifert, *ibid.* **58**, 7260 (1998).
[18] A. Di Carlo, Phys. Status Solidi B **217**, 703 (2000), and reference therein.
[19] J.C. Slater and G.F. Koster, Phys. Rev. **94**, 1498 (1954); D. Chadi and M.L. Cohen, Phys. Status Solidi B **68**, 405 (1975); W.A. Harrison, Phys. Rev. B **8**, 4487 (1973); J. A. Majewski and P. Vogl, *The Structure of Binary Compounds*, edited by F.R. de Boer and D.G. Pettifor (Elsevier, Amsterdam, 1989).
[20] P. Vogl, H.P. Hjalmarson, and J.D. Dow, J. Phys. Chem. Solids **44**, 365 (1983).
[21] J-M. Jancu, R. Scholz, F. Beltram, and F. Bassani, Phys. Rev. B **57**, 6493 (1998); R. Scholz, J-M. Jancu, and F. Bassani, in *Tight-Binding Approach to Computational Materials Science*, edited by P.E.M. Turchi, A. Gonis, and L. Colombo, Mater. Res. Soc. Symp. Proc. **491** (Materials Research Society, Pittsburgh, 1998), p. 383.
[22] Aldo Di Carlo, S. Pescetelli, M. Paciotti, P. Lugli, and M. Graf, Solid State Commun. **98**, 803 (1996).
[23] W. Kohn, in *Solid State Physics: Advances in Research and Applications*, edited by F. Seitz and D. Turnbull (Academic, New York, 1957), Vol. 5, p. 257.
[24] M. Altarelli, in *Heterojunction and Semiconductor Superlattices*, edited by G. Allan, G. Bastard, N. Boccara, M. Lannoo, and M. Voos (Springer, Berlin, 1986), p. 12.
[25] G.T. Einevoll and L.J. Sham, Phys. Rev. B **49**, 10 533 (1994).
[26] B.A. Foreman, Phys. Rev. Lett. **80**, 3823 (1998); **81**, 425 (1998); Phys. Rev. B **54**, 1909 (1996).
[27] L.-W. Wang, A. Franceschetti, and A. Zunger, Phys. Rev. Lett. **78**, 2819 (1997).
[28] S. Froyen, J. Phys.: Condens. Matter **8**, 11 029 (1996).
[29] L.-W. Wang and A. Zunger, Phys. Rev. B **59**, 15 806 (1999).
[30] A. Baldereschi, S. Baroni, and R. Resta, Phys. Rev. Lett. **61**, 734 (1988).
[31] A. Trellakis, A.T. Galick, A. Pacelli, and U. Ravaioli, J. Appl. Phys. **81**, 7880 (1997).
[32] M. V. Fischetti and S. E. Laux, IBM DAMOCLES Project. Web site: http://www.research.ibm.com/0.1um/laux
[33] Such approximation should be relaxed if thin oxide effects are investigated.
[34] S. Froyen, Phys. Rev. B **39**, 3168 (1989).
[35] K.A. Mader and A. Zunger, Phys. Rev. B **50**, 17 393 (1994).